

A CRACK CLOSURE MODEL FOR BRITTLE ROCK SUBJECTED TO COMPRESSIVE SHEAR LOADING^①

Chen Feng, Sun Zongqi and Xu Jicheng

*Opening Lab of Mechanics, Central South University of Technology,
Changsha 410083, P. R. China*

ABSTRACT Crack closure in brittle materials subjected to compressive-shear loading is studied to gain insight into compressive-shear failure mechanism. An analytical wing crack model for the stress intensity factors is developed in the light of superimposition principle. The model can be successfully used to predict out-of-plane initiation and extension. Comparison shows that the K_I values at wing crack tips obtained by the present method agree well with the exact solution proposed by Horii and Nemat-Nasser. The comparison with other approximate model is also given.

Key words crack closure compressive-shear loading stress intensity factor

1 INTRODUCTION

Compression-shear fracture of rock was investigated by many researchers, Rao *et al*^[1] studied this failure mode using four point bending specimen.

Since recent two decades, interest in the mechanical response of brittle rock to natural loadings has motivated the study of failure mechanism of brittle rock under compressive loading, which is one of the major loading modes subjected by these kinds of materials. The failure mechanism of brittle rock under compression is significantly different from that of tensile failure. Three steps are usually included in overall failure of brittle rock subjected to compressive-shear loading.

(1) Single crack initiates from pre-existed notch or crack via kinking when the remote compressive stresses reach the critical value.

(2) The further growth of wing crack leads to the interaction and linkage of cracks.

(3) Crack unstable growth begins when the crack length reaches its critical value and will finally lead to overall failure.

A solution to a single crack initiation and

extension under remote compressive loading is the first step toward understanding compressive-shear failure. Present study is concerned with the first step, in which non-planar extension (kinking) and closure of a single crack in brittle rock are investigated.

The crack closure and kinking caused by compressive loading, due to its importance, is investigated widely by many authors. These problems have been tackled by Nemat-Nasser and Horii^[2-4], who calculated the stress intensity factors (SIF) at the wing crack tips via numerical solution to a singular integral equation. Though their results can be considered as an exact solution and provide a comparison for the expression derived in this paper, it is still not easy to be used in practical calculation. The earlier expression for stress intensity factor at wing crack tips, K_I^{wing} , was developed by Cotterell and Rice^[5] using a perturbation technique for slightly curved cracks, however, it didn't include the influence of crack closure on SIF at wing crack tips.

Some approximate expressions for stress intensity factors at wing crack tips have been developed in recent years. Paul^[6] suggested an ap-

① Project 49272151 supported by the National Natural Science Foundation of China

Received Jan. 22, 1998; accepted Feb. 4, 1999

proximate expressions for wing crack SIF calculation. Though the stress intensity factors obtained by this model have the same tendency as those calculated by Nemat-Nasser and Horii^[2], they differ some what from those given in Ref. [2], particularly for larger wing cracks^[6]. Recently, Baud *et al*^[7] proposed a different approximate method for wing crack extension, their method gives only the variation of mode I SIFs at wing crack tips versus wing crack length l/a , and is also not easy to be used in practical computation. In this paper, a high precision wing crack SIF model is developed based on superimposition principle, the closed-form expression for SIFs at wing crack tips is derived with the assumption that wing crack propagation occurs at a maximum constant critical K_I^{wing} , which is equivalent to that K_{II}^{wing} tends to zero^[5]. The obtained expression allows one to calculate normalized stress intensity factors at wing crack tips.

On the other hand, maximum hoop stress criterion can be very successfully used to predict crack initiation in brittle rock, which holds that when the maximum circumferential stress near crack tip reaches a critical value, wing cracks develop as the initial propagation occurs. The kinking angle θ is convinced by both theoretical analysis and experiments to be about 70.5° from the original main crack direction even under pure mode II loading. This is equivalent to that when wing cracks initiate and K_{II} at wing tips tends to zero. Thus, in the following derivation, only mode I stress intensity factor at wing crack tips is considered to contribute wing crack initiation. The influence of different parameters such as Coulumb's friction coefficient μ , confining pressure σ_1 and main crack orientation β , is also considered in the present investigation.

2 DERIVATION OF WING CRACK SIF MODEL

We consider an infinite body containing a single crack subjected to remote uniform biaxial compression, σ_1 , σ_2 , see Fig.1. The crack of length $2a$ is oriented at an angle β with respect to x -axis. The body is under plane strain condi-

tion. In the light of linear elastic fracture mechanics (LEFM), mode I SIFs at wing crack tips in Fig.1 can be written as follows^[6]:

$$K_I^{\text{wing}} = K_I^{\text{isol}} + K_I^{\text{infl}} \quad (1)$$

where K_I^{wing} is the SIFs at wing crack tips, K_I^{isol} is the SIFs wing crack tips when an isolated crack^[6] of length l exists in an infinite body subjected to the same remote compressive stress σ_1 , σ_2 . The graphical explanation of Eqn.(1) is illustrated in Fig.2. K_I^{infl} in Fig.2(c) denotes the contribution of main crack to wing crack SIFs, which consists of two kinds of influences.

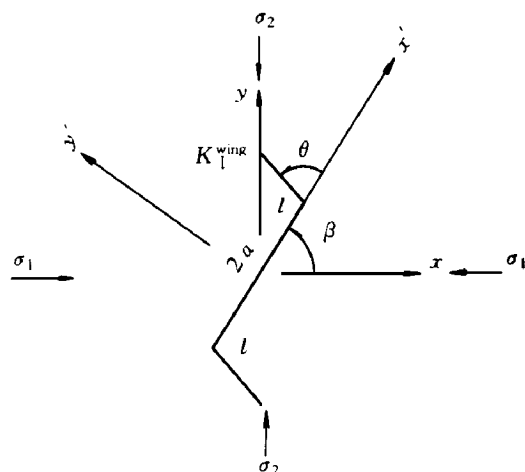


Fig.1 Crack geometry and coordinate arrangement

In Fig.2(b) l is the length of one isolated wing crack in an infinite plate subjected to the same remote stresses as shown in Fig.2(a). τ_{eff} in Fig.2(c) denotes the effective shear stress experienced by main crack, which is induced by remote compressive stresses σ_1 , σ_2 . It is assumed that main crack is closed by remote compressive stress σ_1 and σ_2 , friction caused by sliding of main crack faces can then be calculated through effective shear stress, which can be written as:

$$\tau_{\text{eff}} = \tau + \mu |\sigma| \quad (2)$$

where τ and σ are shear and normal stresses experienced by inclined main crack, μ is the friction coefficient. The sign of friction force $\mu |\sigma|$ is always taken to oppose the shear stress τ . For the present load case: $\sigma_2 < \sigma_1 < 0$, τ is negative (along negative direction of x axis), friction

force μq is then chosen to be positive. For the main crack of length $2a$ oriented at an angle β with respect to x axis, as shown in Fig.1, the shear and normal stresses on main crack plane under remote uniform biaxial compression q_1 and q_2 can be easily calculated as follows:

$$\tau = \frac{1}{2} (q_2 - q_1) \sin 2\beta \quad (3a)$$

$$\sigma = \frac{1}{2} [(q_2 + q_1) + (q_2 - q_1) \cos 2\beta] \quad (3b)$$

Substituting Eqn.3 into Eqn.(2) gives

$$\tau_{\text{eff}} = \frac{1}{2} (q_2 - q_1) \sin^2 \beta + \mu \left| \frac{1}{2} (q_2 + q_1) + \frac{1}{2} (q_2 - q_1) \cos 2\beta \right| \quad (4)$$

For $q_2 < q_1 < 0$, the wing cracks will initiate at an positive angle $\theta > 0$ (anti-clockwise, see Fig. 1), τ_{eff} is negative, otherwise the main crack faces will be self-locked and can not slide.

The contribution of main crack to model I SIFs at wing crack tips consists of two parts, one is the geometrical influence and the other is stress influence. Thus Fig.2(c) can be further decomposed, graphical explanation of main crack influence in Fig.2(c) is plotted in Fig.3.

We consider first the geometrical influence of main crack on wing crack. Since the existence of main crack tends to lengthen the wing crack system by the amount of $2l_{\text{eq}}$, which can be calculated by “projecting” main crack of $2a$ in the wing crack orientation, see Fig.3(b), thus, the total length of wing crack system now becomes $2l + 2l_{\text{eq}}$. The equivalent crack length $2l_{\text{eq}}$ in

Fig.2 Superimposition of model I SIFs at wing crack tips

Fig.3 Analysis of geometrical and stress influence of main crack on mode I SIFs at wing crack tips

Fig.3(b) can be derived easily using sine theorem in triangle ABC of Fig.3(b) as follows:

$$\frac{AC}{\sin \beta} = \frac{AB}{\sin[\pi - (\beta + \theta)]}$$

Noting that $AB = 2a$, $AC = 2l_{eq}$, there is following equation:

$$l_{eq} = \frac{a \sin \beta}{\sin(\beta + \theta)} \quad (5)$$

where β is the main crack orientation, θ is kinking angle of wing cracks. We now determine the stress influence of main crack on wing crack, for this purpose, the effective shear stress τ_{eff} subjected by main crack can be transferred to the equivalent crack $2l_{eq}$ with the same orientation as shown in Fig.3(a). It is clear that only the normal component of τ_{eff} , denoted by σ_{eq} , which is perpendicular to l_{eq} , serves as a wedging force for the wing cracks.

In order to calculate wedging stress σ_{eq} , which acts on the equivalent wing crack system, τ_{eff} is resolved in two components, with one perpendicular and another parallel to the equivalent wing crack system $2l + 2l_{eq}$, as shown in Fig.3(c). From the geometrical relation in Fig.3(b), and noting that τ_{eff} is negative under present remote stress σ_1 , σ_2 , we obtain tensile wedging stress:

$$\sigma_{eq} = -\tau_{eff} \sin \theta \quad (6)$$

Since only the normal component of effective shear stress contributes to model I SIFs at wing crack tips, the total influence of main crack, K_I^{infl} , can then be obtained using load case illustrated in Fig.4(a), which is equivalent to a central crack of length $2l + 2l_{eq}$ in an infinite

plate subjected to a normal stress σ_{eq} on the middle part of wing crack system, see Fig.4(b). The stress intensity factors K_I^{infl} of this load case can be obtained by integrating Wastergaard solution for SIFs. Wastergaard stress intensity factor solution for the load case shown in Fig.4(c) can be written as:

$$K_I = \frac{2p}{\sqrt{\pi}} \frac{\sqrt{a}}{\sqrt{a^2 - b^2}} \quad (7)$$

where p is concentrated force acting at the points of $x = \pm b$ on the crack faces, see Fig.4(c). Applying Eqn.(7) to load case Fig.4(b), which represents the influence of main crack on wing crack SIFs, yields K_I^{infl} . This can be easily done by substituting p , b and a in Eqn.(7) with $\sigma_{eq} dx$, x and $l + l_{eq}$, respectively, and then integrating Eqn.(7) with respect to x from 0 to l_{eq} , which gives the main crack influence, K_I^{infl} as follows:

$$K_I^{infl} = 2\sigma_{eq} \sqrt{\frac{l + l_{eq}}{\pi}} \sin^{-1} \left[\frac{l_{eq}}{l + l_{eq}} \right] \quad (8)$$

Substituting Eqns.(5) and (6) into Eqn.(8) yields:

$$K_I^{infl} = -2\tau_{eff} \sin \theta \sqrt{\frac{l + a \sin \beta / \sin(\beta + \theta)}{\pi}} \times \sin^{-1} \left[\frac{a \sin \beta / \sin(\beta + \theta)}{l + a \sin \beta / \sin(\beta + \theta)} \right] \quad (9)$$

where τ_{eff} is effective shear stress subjected by main crack faces.

For the stress intensity factors at isolated wing crack tips in Fig.2(b), it is straightforward to calculate K_I^{isol} as follows:

$$K_I^{isol} = \frac{1}{2} \sqrt{(\sigma_2 + \sigma_1) +}$$

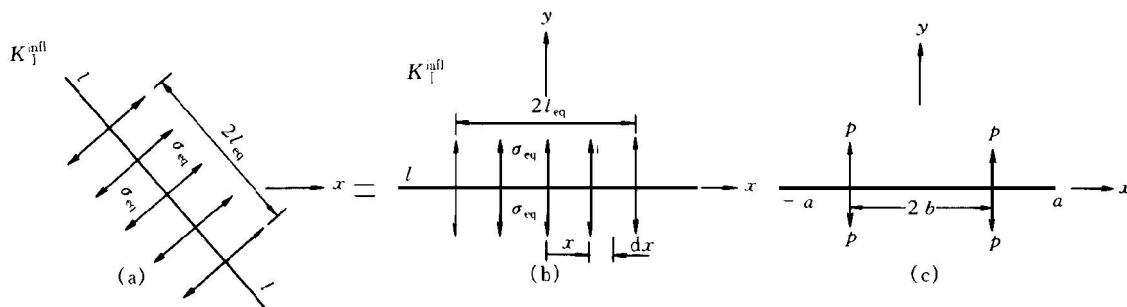


Fig.4 Graphical illustration for K_I^{wing} calculation

$$+ (\sigma_2 - \sigma_1) \cos 2(\beta + \theta) \Big] \sqrt{\frac{\pi l}{2}} \quad (10)$$

Substituting Eqns.(9) and (10) into Eqn.(1) gives

$$K_I^{\text{infl}} = -2 \tau_{\text{eff}} \sin \theta \sqrt{\frac{l + \alpha \sin \beta / \sin(\beta + \theta)}{\pi}} \times \\ \sin^{-1} \left[\frac{\alpha \sin \beta / \sin(\beta + \theta)}{l + \alpha \sin \beta / \sin(\beta + \theta)} \right] + \\ \frac{1}{2} [(\sigma_2 + \sigma_1) + \\ (\sigma_2 - \sigma_1) \cos 2(\beta + \theta)] \sqrt{\frac{\pi l}{2}} \quad (11)$$

Eqn.(11) contains two parts, the second part represents an isolated wing crack influence on SIFs at wing crack tips, which is exactly the same as that derived by Paul^[6]. However, the first part of Eqn(11), which denotes the main crack influence on SIFs at wing crack tips, is completely different from that derived by Paul^[6]. Graphical explanation of Eqn.(11) is plotted in Fig.5.

In order to verify the proposed SIF model at wing crack tips, Eqn.(11) is compared with the results obtained by Nemat-Nasser and Horii^[2] for the case of $\sigma_1 = 0$, $\beta = 54^\circ$ and $\mu = 0.3$. In Fig.5, the normalized mode I stress intensity factors based on Eqn.(11) are plotted as a function of wing crack angle θ . Results from Nemat-Nasser and Horii^[2] are also plotted in Fig.6 for comparison. Noting that the symbols used by Nemat-Nasser and Horii in Fig.6^[2]: θ , c , ν and σ_1 are equivalent to θ , α , $90^\circ - \beta$ and σ_2 used in the present derivation, Fig.5 and Fig.6 can then be directly compared. Comparison between present results and those obtained by Nemat-Nasser and Horii^[2], shows that proposed wing crack SIF model is quite consistent with the exact solution given in Ref.[2], especially for longer wing crack, this greatly improved approximate model proposed by Paul^[6].

Normalized wing crack stress intensity factors calculated by different wing crack models for the cases of $l/a = 0.5$ and $l/a = 1$ are also plotted in Fig.7 for comparison.

It is clear from Fig.7 that the precision of wing crack SIFs calculated by our expression is higher than approximate model derived by

Paul^[6], especially for larger wing cracks. Although present model underestimates the maximum normalized model I SIFs at wing crack tips, it is still much closer to the exact solution

Fig.5 Normalized mode I SIFs at wing crack tips versus kinking angle θ for indicated wing crack length obtained by present model ($\beta = 54^\circ$, and $\mu = 0.3$)

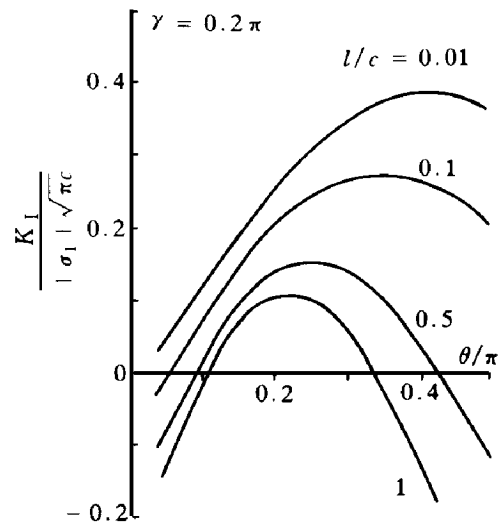


Fig.6 Normalized mode I SIFs as a function of kinking angle θ for indicated crack length and $\mu = 0.3$ given by Nemat-Nasser and Horii^[2], symbols ν , c and σ_1 in Fig.6 are equivalent to $90^\circ - \beta$, a , and σ_2 in Fig.5

Fig.7 Comparison of different approximate wing crack models
for normalized model I SIF

1 — Ref.[6]; 2 — Ref.[2]; 3 — In this paper

obtained by Nemat-Nasser and Horii^[2] than the model derived by Paul^[6].

3 CONCLUSIONS

An analytical mode I SIF formula at wing crack tips for brittle rock is developed based on superimposition principle. The expression for stress intensity factors at wing crack tips permits one to calculate the values of K_I^{wing} as a function of applied remote stress σ_1 , σ_2 , friction coefficient μ and main crack inclination angle β . The proposed expression is more convenient for wing crack initiation and extension analysis than numerical method by Nemat-Nassar and Horii^[2]. Although the maximum K_I^{wing} values for short wing crack ($l/a = 0.01$ and 0.1) do not reach within $\theta < 0.5\pi$, the precision of K_I^{wing} for small kinking angle ($\theta < 0.4\pi$) is still very high. Comparison shows that the precision of K_I^{wing} for

$l/a = 0.5$ and 1 obtained by present model is consistent well with the exact numerical solution by Horii Nemat-Nasser^[4], and higher than other approximate models.

REFERENCES

- 1 Rao Qiuhua, Sun Zongqu and Xu Jicheng. The Chinese J of Nonferrous Metals, (in Chinese), 1997, 1 (Suppl.2): 115-117.
- 2 Nemat-Nasser S and Horii H. J Geophys Res, 1982, 87(88): 6805 - 6821.
- 3 Horii H and Nemat-Nasser S. Phil Trans RSOL Land A, 1986, 319: 337 - 374.
- 4 Horii H and Nemat-Nasser S. J Geophys Res, 1985, 90(B4): 3105 - 3125.
- 5 Cotterell B and Rice J R. Int J Fracture, 1980, 16: 155 - 169.
- 6 Paul S S. Eng Mech, 1984, 20(3): 463 - 473.
- 7 Baul P, Reuschle and Charle P. Int J Rock Mech Sci & Geomech Abstr, 1996, 33(5): L539 - 542.

(Edited by He Xuefeng)